Precipitation Effects for X- and Ka-band SAR

Andreas Danklmayer
DLR, Microwaves and Radar Institute, Germany

Madhukar Chandra
Chemnitz University of Technology, Dept. of Microwave Engineering and Photonics, Germany

Abstract

Space-borne Synthetic Aperture Radar (SAR) imaging is often considered to possess both day/night and all weather operational capabilities. Whereas the first argument is true since we are dealing with an active sensor; the second does not hold in cases for which the operating frequencies are above 3 GHz. Indeed, the SAR performance can be significantly affected by atmospheric effects (losses), especially at unfavourable weather conditions. The principal reasons for the restriction on the use of these higher frequencies can be found in clear air losses (water vapour and oxygen), cloud attenuation and attenuation due to precipitation, primarily rain.

1 Tropospheric Effects

The troposphere, as the lowest part of the Earth's atmosphere, reaches from the surface to approximately 12 km above ground and causes, amongst other effects, attenuation of traversing signals due to hydrometeors (rain, snow, hail), atmospheric gases, fog and clouds [2]. Except at low elevation angles, the attenuation of frequencies below 1 GHz is negligible. Insignificant contributions to the attenuation will be obtained for frequencies up to 10 GHz due to fog and non-precipitating clouds. However the transmission spectrum exhibits peaks for frequencies around 22 GHz and 60 GHz due to molecular resonances from gases i.e. water vapour and oxygen. Whereas absorption effects due to atmospheric gases are present constantly and everywhere, attenuation due to condensed water in the form of precipitation, clouds and fog is infrequent and is limited to certain areas. Attenuation consists of two physical processes: the reduction of the wave's energy due to the heating of the water particles and, the scattering of energy away from the main direction of propagation. Further details on the assessment of atmospheric effects on SAR images can be found in [3].

1.1 Modelling of Attenuation and Backscattering in SAR images

For the modelling of the attenuation and backscattering effects in SAR images, **Figure 1** is clarifying the underlying geometry [4]. The diagram provided at the bottom of **Figure 1** shows the qualitative variation of the normalised radar cross section (NRCS) due to the idealised rain cell. The detailed modelling and calculation is provided in the following two sections.

One of the major problems affecting microwave and millimetre wave bands for terrestrial and space-borne radars is the attenuation through rain [2]. A convenient way to describe the rain intensity is the so called rainfall-rate or rain-rate given in millimetres per hour. This quantity refers to a certain flux of rain towards the surface of the Earth and may be measured e.g. by gauges or weather radars. A widely acceped empirical relation of the form

$$\gamma(x,t) = a \cdot R^b \tag{1}$$

between specific attenuation $\gamma(x,t)$ and rain rate R is used to calculate the specific attenuation for a given rain rate [2, 5]. The parameters a and b are dependent on the radio frequency, the raindrop size distribution, the polarization and other factors [5].

After [2], the total attenuation for a given instant of time can be obtained by adding up the specific attenuation along the path of propagation using the following expression

$$A(t) = \int_0^{2h} \gamma(x,t)dx \tag{2}$$

where

$A(t)$	... total attenuation for given time instant t
t	... time
h	... path length
$\gamma(x,t)$	... specific attenuation
x	... position along the path of propagation

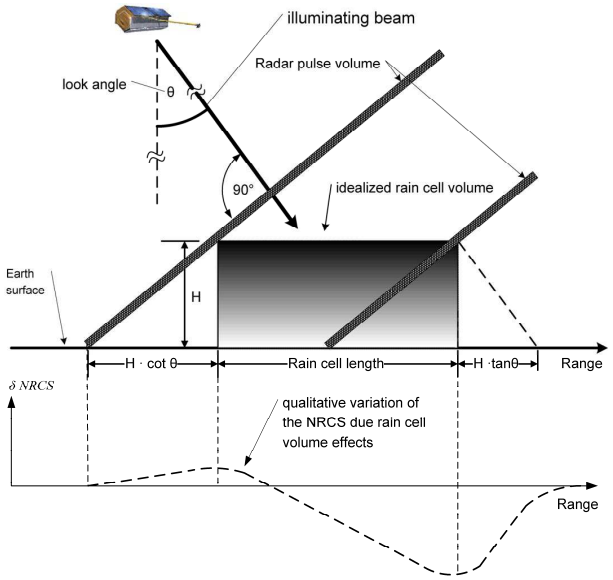

Figure 1: A depiction of a SAR imaging scenario of an idealised rain cell. In the diagram the qualitative variation of the NRCS due to the rain cell volume effects is given. A combination of backscattering and attenaution can occur, where qualitatively the backscattering due to rain is the minor effect and attenuation the major [4]

The specific attenuation along the slant path of propagation has to be known. However, detailed knowledge of the medium through which the signal propagates is rather limited and the temporal and spatial variation of the medium require assumptions and some modelling. In the case of precipitation we may have some idea about the thermodynamic phase (ice, water, melting band) but no precise information. Using the calculated values for the specific attenuation in X-band provided in diagram **Figure. 2** for a 5 km long path through a heavy tropical convective rain (70 mm/h and more) suggests a 20 – 30 dB attenuation, which was confirmed by comparing the backscattering coefficient of affected and non–affected region from data takes acquired by TerraSAR-X over Brazilien rain forest.

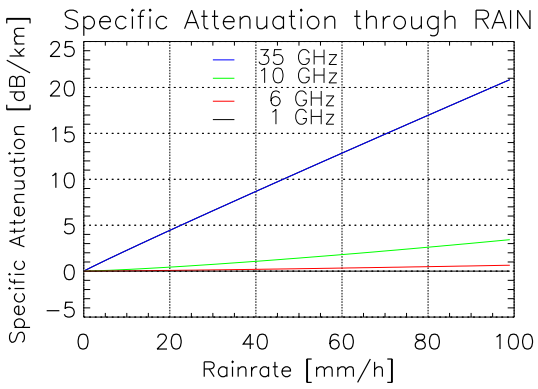

Figure 2: A plot of the specific attenuation given in units of dB/km versus the rain rate in units of mm/h for four different frequencies (1, 6, 10 and 35 GHz) after the ITU Model Recommendation 838 (2003).

1.2 Modelling of the Attenuation under Rain Conditions for Ka-band

For the calculations of the rain rate to cause visible attenuation in Ka-band SAR images, a simple model shown in **Figure 3** [4], is used. A reasonable height of 4 km is assumed, as well as a homogenous rain rate for the modelled cell. The incidence angle of the propagating signals was chosen 30^o. With the help of (1) and by using the regression coefficients in Table 1, the specific attenuation was calculated. These values are given in Table 1.2. Finally, the values for the two-way path attenuation for different rain rates (5, 50 and 100 mm/h) can be found in Table 3. As a total two-way attenuation of 25 dB becomes visible in SAR images in X-band it is of interest which rain rate is necessary to cause such an attenuation for Ka-band (35 GHz) frequencies. To this end, the following equation is applied

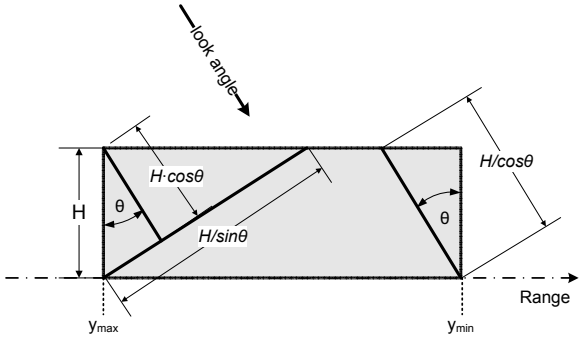

Figure 3: The structure of an idealised rain cell used for the calculation in Section 1.2.

$$\gamma(t) = \frac{A(t)}{2 \cdot \frac{H}{\cos(\theta)}} \qquad \text{[dB/km]} \qquad (3)$$

where the rain rate is found using (1) with the according parameters a and b for Ka-band.

$$R = \sqrt[b]{\frac{\gamma(t)}{a}} \qquad (4)$$

Table 1: Regression coefficients used for the calculation of the specific attenuation cf. (1)

Frequency	DSD			
	Mar. Palmer		Joss Thunderst.	
	a	b	a	b
X-Band (10 GHz)	0.0136	1.15	0.0169	1.076
Ka-Band (35 GHz)	0.268	1.007	0.372	0.783

First calculations using the parameters of the idealised rain cell of 4 km and using 25 dB of total two-way attenuation, assuming the Marshall Palmer Parameters for Ka-band attenuation deliver a rain rate close to 10 mm/h. This simple example demonstrates that such rain rates are fully capable to distort Ka-band SAR measurements to a visible extent. In **Figure 4** the range of values for attenuation and rain rate are extendent and the diagram shows the two-way attenuation versus the rain rate for different incidence angles at Ka-band. Similar information is provided for X-band frequencies in **Figure 5**. In addition to the aforementioned simple assumptions of a homogenous rain cell with constant precipitation may be somehow optimistic, since a melting layer precipitation may severly increase the total path attenuation.

Table 2: Specific Attenuation $[dB/km]$

Rainrate	**Specific Attenuation**	
[mm/h]	10 GHz	35 GHz
5	0.08	1.31
50	1.22	7.95
100	2.4	13.69

Table 3: Maximum Attenuation for modelled rain cell $[dB]$

Rainrate	**Max. Attenuation**	
[mm/h]	10 GHz	35 GHz
5	0.739	12.1
50	11.26	73.43
100	22.17	126.46

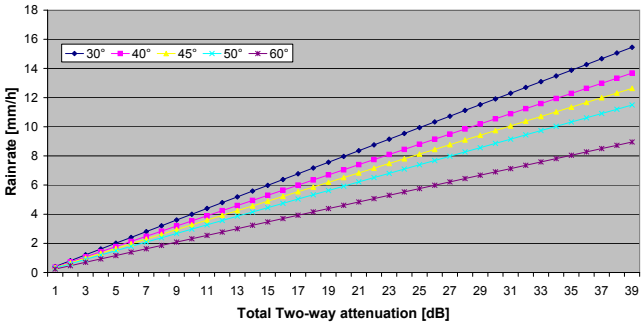

Figure 4: A diagram of the two-way path attenuation and the corresponding rain rate for the modelled rain cell of 4 km height (Fig. 3) at Ka-band (35 GHz), for different look angles.

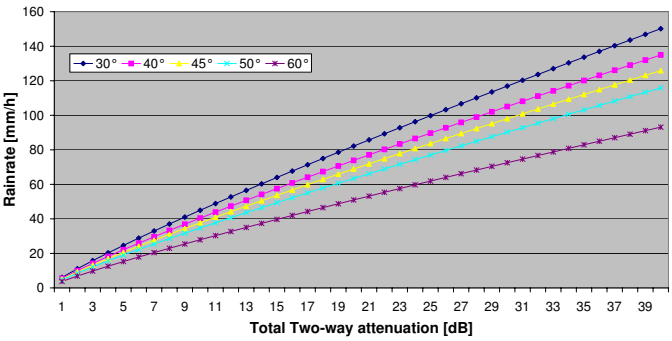

Figure 5: A diagram of the two-way path attenuation and the corresponding rain rate for the modelled rain cell (Fig. 3) at X-band (10 GHz), for different look angles.

1.3 Consideration of Backscattering effects in SAR imaging

The radar response (backscattering) from hydrometeors is determined by the raindrop size, shape, density, orientation, and temperature. Furthermore, the backscattering depends on the polarization of the wave interacting with the precipitation media. The theoretical concept that describes the scattering from a dielectric sphere was established by Mie in 1908. The relation to estimate the backscatter cross section of a volume of small particles by assuming the well-known Rayleigh approximation (the diameters D of the raindrops are much smaller than the wavelength λ) is given as

$$\sigma_b = \frac{\pi^5}{\lambda^4}|K|^2 \sum_{i=1}^{N} \cdot D_i^6 \tag{5}$$

where

$$K = \frac{m^2 - 1}{m^2 + 2} \tag{6}$$

and m is the complex index of refraction of the scattering particle. The summation term for a distribution of particles can be given as

$$\hat{Z} = \int N(D_e) D_e^6 dD_e \qquad [\mathrm{mm}^6/\mathrm{m}^3] \tag{7}$$

where $\hat{Z}$ is termed the reflectivity factor, D_e is the diameter of each droplet and $N(D_e)$ is the number of droplets per unit volume.

$$N(D_e) = N_0 e^{-\lambda_d D_e}; \quad \lambda_d = 4.1 \quad R^{-0.21} \tag{8}$$

where N_0 and λ_d are the parameters defining the drop size distribution (DSD). For the special case of the Marshall-Palmer distribution the parameter N_0 is given as 8000 in m^{-3} mm^{-1} , and λ_d $[\mathrm{mm}^{-1}]$ is related to the rainfall intensity R [mm/h] as shown in Eq.8.
Note that $\hat{Z}$ is commonly given in logarithmic units according to

$$Z = 10 \cdot log_{10}\hat{Z} \qquad [dBZ] \tag{9}$$

As a practical basis for estimating the precipitation intensity directly from the measured reflectivity factor in still air, the following relation is used

$$\hat{Z} = a_1 \cdot R^{b_1} \tag{10}$$

The parameters a_1 and b_1 are dependent on the frequency of the interacting EM waves and on the rain intensity R as well as the DSD. Furthermore, regional-dependent variations due the rain type do exist. A number of $Z - R$ relations were established by many research efforts. A careful selection of the coefficients has to be performed by considering the appropriate conditions and respective parameters. The power law in (10) provides an analogy to the calculations of the specific attenuation using (1) given in Section 1.2.

For the case of SAR, it can be concluded that the backscattering due to hydrometeors is the minor effect and attenuation due to the precipitation volume is dominating, which is supported by recent measurements of TerraSAR-X.

It has been observed that backscattering due to precipitation can easily enhance the backscattering about 5 dB compared to unaffected regions of the image.

2 Conclusions

It has been found that attenuation due to rain is the dominating effect, together with backscattering from precipitation for higher frequency bands such as X- and Ka-band. Since the effects of backscattering and attenuation is interconnected to each other it is sufficient to consider at least the major disturbance (=attenuation through rain) in order to flag an affected SAR image. A model to quantify propagation effects in SAR images has been presented, which allows for a quantitative assessment of the pertinent effects. Depending on the climatic region on Earth, the availability of the investigated Ka-band system will vary. Assuming a 5 dB acceptance of the attenuation due to rain, which corresponds to 2 mm/h at 30° incidence angle for the modelled rain cell used in this paper, the availability will be better than 98 % for the European regions and better than 95 % for rain-forest in Brazil.

Acknowledgements

This research was partly financed by ESA under contract No. 21876/08/NL/ST/al "Precipitation effects for Ka-band SAR".

References

[1] Danklmayer,A.: "Precipitation Effects for Ka-band SAR, ESA-ESTEC/ Final Report Contract No. 21876/08/NL/ST/al, 2009"

[2] Crane, R. K. *Electromagnetic wave propagation through rain*. John Wiley and Sons, 1996.

[3] Danklmayer, A.; Döring, B.; Schwerdt, M.; and M. Chandra: "Assessment of Atmospheric Effects in SAR Images," *IEEE Transaction on Geoscience and Remote Sensing*, 2009, vol. 47, no. 10, pp. 3507-3518, October 2009,

[4] Melsheimer, C.: *Signaturen von Regen in Radaraufnahmen des Meeres*. Aachen: Shaker Verlag, 1998.

[5] Olsen,R. L.; Rogers, D. V.; and D. B. Hodge: "The $a \cdot R^b$ relation in calculation of rain attenuation," *IEEE Transactions on Antennas and Propagation*, vol. 26, no. 2, pp. 318–329, 1978.

[6] Specific Attenuation Model for Rain for Use in Prediction Methods, 2005. *ITU-Recommendation P. 838-3.*

[7] D'Addio, S.; Ludwig, M.; "Rain Impact on Sensitivity of Ka-band Scan-on-Receive Synthetic Aperture Radars," in *IEEE International Geoscience and Remote Sensing Symposium, (IGARSS)* 2008, vol 3, 7-11 July 2008 Page(s):III - 1174 - III - 1177, Boston, US